

FINGERPRINT MOSAICKING

Anil Jain and Arun Ross

Michigan State University
East Lansing, MI, USA 48824
{jain, rossarun}@cse.msu.edu

ABSTRACT

It has been observed that the reduced contact area offered by solid-state fingerprint sensors does not provide sufficient information (e.g., number of minutiae) for high accuracy user verification. Further, multiple impressions of the same finger acquired by these sensors, may have only a small region of overlap thereby degrading the matching performance of the verification system. To deal with this problem, we have developed a fingerprint mosaicking scheme that constructs a composite fingerprint template using multiple impressions. A composite template reduces storage, improves matching time and alleviates the problem of template selection. In the proposed algorithm, two impressions (templates) of a finger are initially aligned using the corresponding minutiae points. This alignment is used by a modified version of the well-known iterative closest point algorithm (ICP) to compute a transformation matrix that defines the spatial relationship between the two impressions. The resulting transformation matrix is used in two ways: (a) the two templates are stitched together to generate a composite image. Minutiae points are then detected in this composite image; (b) the minutia maps obtained from each of the individual impressions are integrated to create a larger minutia map. Our experiments show that a composite template improves the performance of the fingerprint matching system by $\sim 4\%$.

1. INTRODUCTION

Fingerprint-based verification systems have gained immense popularity due to the high level of uniqueness attributed to fingerprints and the availability of compact solid-state fingerprint sensors that can be easily embedded into a wide variety of devices requiring user-authentication (e.g., laptops, cellular phones). The solid-state sensors, however, sense only a limited portion of the fingerprint pattern present in the tip of the finger. The amount of information (e.g., number of minutiae points) that can be extracted from such partial prints is substantially lower compared to that which can be extracted from more elaborate prints sensed using an optical sensor or inked prints. For example, the average num-

ber of minutiae points extracted from a Digital Biometrics optical sensor (500×500 image at 500 dpi) is 45 compared to 25 minutiae obtained from a Veridicom solid-state sensor image (300×300 image at 500 dpi). Further, the relatively small overlap between the template and query impressions results in fewer corresponding points and, therefore, higher false rejects and/or false accepts (Figure 1). To address the problem of insufficient information in a single fingerprint template, we use an image mosaicking technique that constructs a more complete fingerprint template using multiple impressions of the same finger. A composite template has the following advantages: (a) In the absence of a composite template, the query image will have to be compared with each of the individual template impressions (of the same finger). Due to the small size of these impressions, the amount of overlap between the query image and any template impression is likely to be small, resulting in a false reject of the query image. A composite template, however, reduces the probability of a false reject. (b) The matching time required to compare the query image with the template is reduced. With the availability of a composite template, only a single comparison is necessary. (c) The quandary of template selection is avoided. As information from multiple templates are integrated into a single composite template, the need to 'weight' the individual templates during the matching process is alleviated.

2. BACKGROUND

Registering fingerprint images is a difficult problem for the following reasons: (a) A fingerprint image may have non-linear plastic distortions due to the effect of pressing a convex elastic surface (the finger) on a flat surface (the sensor). Moreover, these distortions may be present only in certain regions of the sensed image due to the non-uniform pressure applied by the subject. (b) The presence of dirt deposits on the sensor or cuts and bruises on the finger can result in a rather noisy image. Therefore, it becomes difficult to register two fingerprint images that have different amounts of distortion or noise. In order to generate the transformation matrix defining the spatial relationship between two im-

pressions, we use a modified version of the *iterative closest point (ICP)* algorithm which tries to register two surface images given an initial alignment between the two surfaces.

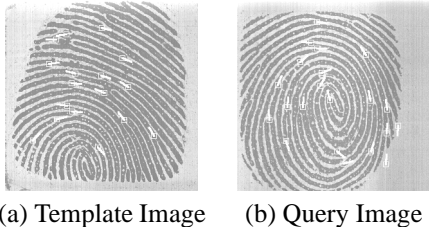


Fig. 1. Limited overlap between two 300×300 impressions of the same finger acquired using the Veridicom sensor. The transformation between these impressions is not known.

The problem of registering multiple 3-D object views has received much attention in the literature (see [1, 2] and the references therein). Consider a rigid transformation \mathcal{T} that relates two range images, R_P and R_Q . The goal of a registration algorithm is to find \mathcal{T} such that the objective function, $D(R_P, R_Q)$, is minimized:

$$D(R_P, R_Q) = \sum_{p \in R_P} \|\mathcal{T}p - f(p)\| \quad (1)$$

where

$$f : R_P \rightarrow R_Q \mid \forall p \in R_P, f(p) \in R_Q.$$

The transformation matrix, \mathcal{T} , expressed in homogeneous coordinates, is shown in Eq. (2). Here α , β and γ are the rotation angles about the x , y and z axes, respectively, and t_x , t_y and t_z are the translation components along the three axes. Thus the matrix \mathcal{T} has 6 independent parameters. In practice, the function f is not known, and therefore the objective function in Eq. (1) has to be replaced by an evaluation function that assumes knowledge of a set of corresponding points in R_P and R_Q . Given N pairs of corresponding points, (p_i, q_i) , $p_i \in R_P$, $q_i \in R_Q$ and $i = 1 \dots N$, one attempts to minimize the evaluation function $E(R_P, R_Q)$ given by,

$$E(R_P, R_Q) = \sum_{i=1}^N \|\mathcal{T}p_i - q_i\|^2. \quad (3)$$

The correspondence points (also known as *control points*) may be selected by extracting higher level features (e.g., edges, corners, points of locally maximum curvature, etc.) from the two surfaces, and looking for correspondences between the two sets of extracted features. In some applications, the control points are manually identified by a domain expert. Given the control points, the evaluation function in Eq (3) can be minimized by simply searching for the global minimum in the 6-dimensional parameter space using an

iterative procedure. Such a procedure, however, does not guarantee convergence to a *global* minimum. To circumvent this problem, the ICP algorithm assumes that an initial approximate transformation, \mathcal{T}^0 , is known. A good starting approximation assures that the global minimum is reached quickly and surely.

Eq. (3) imposes a strict correspondence between points p_i and q_i . If the pair of points selected are incompatible (i.e., they are located on different surfaces in the two images), then an iterative procedure may converge very slowly. To overcome this, the ICP algorithm tries to minimize the distances between points in one image to geometric entities (as opposed to points) in the other. Chen and Medioni [3] attempt to minimize the distance of a point on one surface, to the tangential plane of the corresponding point in the other surface. Thus, we minimize

$$E^k(R_P, R_Q) = \sum_{i=1}^N d_s^2(\mathcal{T}^k p_i, S_j^k), \quad (4)$$

where, d_s is the distance from the point to the plane, and S_j is the tangential plane corresponding to point q_j in image R_Q . Once an initial alignment is provided, the control points are automatically chosen by examining homogeneous regions in the two images. An iterative procedure is adopted to minimize the criterion function (and hence the superscript k in the above equation). Since an approximate initial transformation matrix is assumed to be known, convergence to the global minimum is usually assured, and since there is a relaxation in the condition of strict correspondence between points (Eq. (4)), convergence is faster.

3. FINGERPRINT MOSAICKING

We pose the fingerprint mosaicking problem as a 3-D surface registration problem that can be solved using a modified ICP algorithm. The initial alignment of fingerprint images I_P and I_Q is obtained by extracting minutiae points from each individual image, and then comparing the two sets of minutiae points using an elastic point matching algorithm [4]. The comparison proceeds by first selecting a reference minutiae pair (one from each image), and then determining the number of corresponding minutiae pairs using the remaining sets of points in both the images. The reference pair that results in the maximum number of corresponding pairs is chosen. Let (p_0, q_0) be the reference minutiae pair and let $(p_1, q_1), \dots, (p_N, q_N)$ be the other corresponding minutiae pairs. Here, $p_i = (p_{x_i}, p_{y_i}, p_{z_i}, p_{\theta_i})$ and $q_i = (q_{x_i}, q_{y_i}, q_{z_i}, q_{\theta_i})$, where (x, y) are the spatial coordinates of the minutiae points, z is the intensity of the image at (x, y) and θ is the minutiae orientation. The initial transformation, \mathcal{T}^0 , is computed using Horn's method of unit quaternions [5] that operates on the (x, y, z) values. In this technique, the translation parameters in Eq. (2) are com-

$$\mathcal{T} = \begin{bmatrix} \cos \alpha \cos \beta & \cos \alpha \sin \beta \sin \gamma - \sin \alpha \cos \gamma & \cos \alpha \sin \beta \cos \gamma + \sin \alpha \sin \gamma & t_x \\ \sin \alpha \cos \beta & \sin \alpha \sin \beta \sin \gamma + \cos \alpha \cos \gamma & \sin \alpha \sin \beta \cos \gamma - \cos \alpha \sin \gamma & t_y \\ -\sin \beta & \cos \beta \sin \gamma & \cos \beta \cos \gamma & t_z \\ 0 & 0 & 0 & 1 \end{bmatrix} \quad (2)$$

puted using the centroid of the point sets $(p_{x_i}, p_{y_i}, p_{z_i})$ and $(q_{x_i}, q_{y_i}, q_{z_i})$, and the rotation components are computed using the cross-covariance matrix between the centroid-adjusted pairs of points.

Preprocessing the Fingerprint Image: Since the ICP algorithm uses distances from points to planes, it is very sensitive to rapid and abrupt changes in surface direction. Therefore, the fingerprint images are first median filtered using a 3×3 mask. This operation removes any undesirable “salt-and-pepper” noise that may be present in the valleys of the fingerprint image (which may contribute to abrupt changes in the range image). The intensity values of the median filtered image are then scaled to a narrow range of values $([10, 20])$ to ensure a fairly smooth change in surface direction in the corresponding range image of the fingerprints (Figure 2b).

Fingerprint Segmentation: The purpose of segmentation is to separate the foreground regions (that have ridge and valley information) from the background regions (that have no fingerprint information) in the image. This distinction is necessary to prevent the ICP algorithm from choosing control points in the background regions (due to the homogeneity in intensity in these regions), and erroneously attempting to align the images using such points. The result of the segmentation process is shown in Figure 2c.

Fingerprint as a Range Image: The intensity values are directly used as range values - i.e., the intensity value of the image at the planar coordinate (x, y) is treated as the range value, z , at that location. We now have two range images R_P and R_Q , that are obtained from the corresponding intensity images I_P and I_Q , respectively. Figure 2d illustrates this mapping for a portion of the image in 2c. R_P and R_Q are then subject to the iterations of the ICP algorithm. At each iteration k , the transformation \mathcal{T}^k that minimizes E^k in Eq. (4) is chosen. The process is said to have converged when, $\frac{|E^k - E^{k-1}|}{N} < \epsilon$, where ϵ is some threshold, $\epsilon \approx 0$. The final transformation matrix, $\mathcal{T}^{solution}$, is used in the following two ways: (a) It is used to integrate the two individual images and create a composite image whose spatial extent is generally larger than the individual images. Minutiae points are then extracted from this larger image. (b) The minutiae sets from the individual images are augmented using $\mathcal{T}^{solution}$.

Constructing a Composite Image: The intensity images I_P and I_Q are integrated into a new image I_R by using $\mathcal{T}^{solution}$ to compute the new spatial coordinate of every pixel in I_P . A new minutiae set, \mathcal{M}_{R_1} , is then extracted

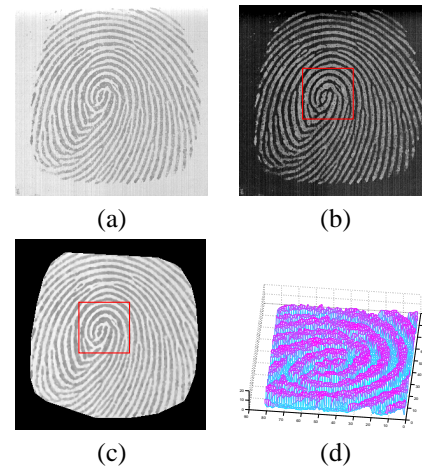


Fig. 2. Mapping an intensity image to a range image. (a) The original intensity image. (b) The intensity image after median filtering and scaling. (c) The segmented intensity image. (d) The range image corresponding to the boxed region (rotated by $\sim 90^\circ$) in (c).

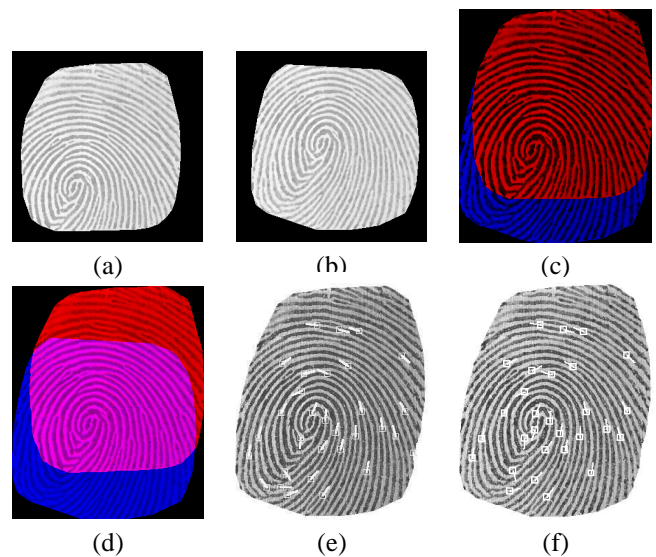


Fig. 3. Composite template construction: (a) First image after segmentation. (b) Second image after segmentation. (c) Initial alignment. (d) Final alignment. (e) Minutiae extracted from mosaicked images. (f) Composite minutiae set obtained after augmenting individual minutiae sets.

from I_R using the algorithm described in [4] (figure 3e).

Augmenting Minutiae Sets: If \mathcal{M}_P and \mathcal{M}_Q refer to the minutiae sets extracted from I_P and I_Q , respectively, then a composite minutiae set, \mathcal{M}_{R_2} , is obtained by augmenting \mathcal{M}_P and \mathcal{M}_Q . The new (x, y) coordinates of \mathcal{M}_P are determined by simply multiplying the old coordinates with $\mathcal{T}^{solution}$ (Figure 3f).¹ The minutiae orientation, θ , is not recomputed.

4. EXPERIMENTAL RESULTS

300 × 300 fingerprint images of 160 different fingers (corresponding to 160 different subjects) were acquired using the Veridicom solid-state sensor. Four different impressions of each of these fingers were obtained over two different sessions separated by a period of one month (2 impressions in each session). The impressions obtained from the first session were used to construct the composite template, while the impressions obtained from the second session were used as query images during the test phase of the experiment. Thus, 160 pairs of images were used to construct minutiae templates \mathcal{M}_{R_1} (extracting minutiae from the mosaicked image) and \mathcal{M}_{R_2} (augmenting individual minutiae sets); the rest of the 320 images were used as query images. This makes the matching problem challenging, since the images used for template construction and the images used for testing the system were acquired at different times. The following table lists a few statistics about the composite image generated using the modified ICP algorithm:

	Avg. Size	Avg. No. Minutiae
Input Image	300 × 300	22
Composite Image	336 × 332	30

Given a minutiae set \mathcal{M}_U (of query image I_U), and the template minutiae sets \mathcal{M}_P , \mathcal{M}_Q , \mathcal{M}_{R_1} and \mathcal{M}_{R_2} , we perform the following comparisons: (a) \mathcal{M}_U with \mathcal{M}_P , (b) \mathcal{M}_U with \mathcal{M}_Q , (c) \mathcal{M}_U with \mathcal{M}_{R_1} , and (d) \mathcal{M}_U with \mathcal{M}_{R_2} . Thus we get a set of four scores corresponding to these comparisons. The Receiver Operating Characteristic (ROC) curves depicting the performance of the four different matchings are shown in figure 4. We observe that the verification performance is affected by the individual impression that is chosen as the template. Thus, comparing \mathcal{M}_U with \mathcal{M}_P results in a different performance than comparing \mathcal{M}_U with \mathcal{M}_Q . This illustrates the problem of template selection during enrollment time. However, when the composite template \mathcal{M}_{R_1} is used, an improved performance is observed compared to using the individual templates. The augmented minutiae template \mathcal{M}_{R_2} , does not result in a substantial improvement in performance as can be seen in this graph.

¹Since I_P is transformed to align with I_Q , this computation has to be done for \mathcal{M}_P only.

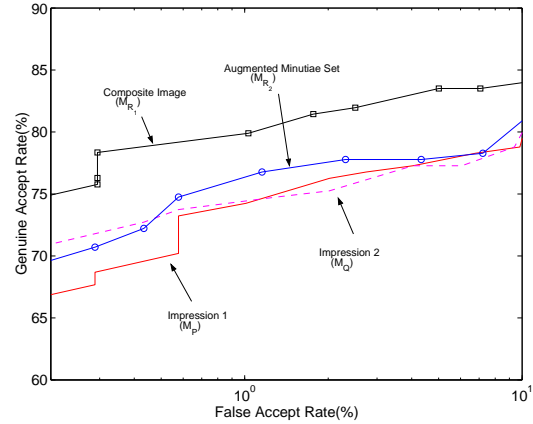


Fig. 4. The Receiver Operating Characteristic (ROC) curves.

5. SUMMARY AND FUTURE WORK

We have described a fingerprint template construction technique, that integrates information available in two different impressions of the same finger, by using a modified ICP algorithm to register the two impressions. Initial experiments indicate that mosaicking the impressions together, and then extracting the (template) minutiae set, results in a better performance of the matching system. Future work involves studying the non-linear deformation of fingerprints, that would aid in better integrating the two impressions. We are also attempting to mosaick three or more impressions to create larger templates.

6. REFERENCES

- [1] Lisa Gottesfeld Brown, “A survey of image registration techniques,” *ACM Computing Surveys*, vol. 24, no. 4, pp. 325–376, 1992.
- [2] Paul J. Besl and Neil D. McKay, “A method for registration of 3-D shapes,” *IEEE Transactions on PAMI*, vol. 14, no. 2, pp. 239–256, February 1992.
- [3] Yang Chen and Gérard Medioni, “Object modelling by registration of multiple range images,” *Image and Vision Computing*, vol. 10, no. 3, pp. 145–155, April 1992.
- [4] Anil K. Jain, Lin Hong, and Ruud Bolle, “On-line fingerprint verification,” *IEEE Transactions on PAMI*, vol. 19, no. 4, pp. 302–314, April 1997.
- [5] Berthold K. P. Horn, “Closed-form solution of absolute orientation using unit quaternions,” *Journal of the Optical Society of America*, vol. 4, no. 4, pp. 629–642, April 1987.